Plant, Cell & Environment

WILEY

Plant, Cell & Environment

ORIGINAL ARTICLE

The RNA m^{6}A Methyltransferase PheMTA1 and PheMTA2 of Moso Bamboo Regulate Root Development and Resistance to Salt Stress in Plant

Huihui Wang[1] | Huiyuan Wang[1] | Yue Jia[2] | Xiaoxia Jin[1] | Hongwei Wu[1] | Siyu Yang[2] | Liangzhen Zhao[2] | Hangxiao Zhang[2] | Lianfeng Gu[2]

[1]College of Forestry, Fujian Agriculture and Forestry University, Fuzhou, China | [2]Fujian Provincial Key Laboratory of Haixia Applied Plant Systems Biology, Basic Forestry and Proteomics Research Center, Haixia Institute of Science and Technology, Fujian Agriculture and Forestry University, Fuzhou, China

Correspondence: Lianfeng Gu (lfgu@fafu.edu.cn)

Received: 1 November 2024 | **Revised:** 1 March 2025 | **Accepted:** 15 March 2025

Funding: This research was funded by the National Natural Science Foundation of China (32371980); Forestry Peak Discipline Construction Project of Fujian Agriculture and Forestry University (72202200205); the National Key R&D Program of China (2021YFD2200505); and S&T Innovation (KFB23180).

Keywords: alternative splicing | HyperTRIBE | m^{6}A methyltransferase | Moso bamboo | MTA | Rice | salt tolerance

ABSTRACT

As the most prevalent RNA modification in eukaryotes, N^6-methyladenosine (m^{6}A) plays a crucial role in regulating various biological processes in plants, including embryonic development and flowering. However, the function of m^{6}A RNA methyltransferase in moso bamboo remains poorly understood. In this study, we identified two m^{6}A methyltransferases in moso bamboo, PheMTA1 and PheMTA2. Overexpression of *PheMTA1* and *PheMTA2* significantly promoted root development and enhanced salt tolerance in rice. Using the HyperTRIBE method, we fused *PheMTA1* and *PheMTA2* with *ADARcd*^{E488Q} and introduced them into rice. RNA sequencing (RNA-seq) of the overexpressing rice identified the target RNAs bound by PheMTA1 and PheMTA2. PheMTA1 and PheMTA2 bind to *OsATM3* and *OsSF3B1*, which were involved in the development of root and salt resistance. Finally, we revealed the effects of transcription or alternative splicing on resistance-related genes like *OsRS33*, *OsPRR73*, *OsAPX2* and *OsHAP2E*, which are associated with the observed phenotype. In conclusion, our study demonstrates that the m^{6}A methyltransferases PheMTA1 and PheMTA2 from moso bamboo are involved in root development and enhance plant resistance to salt stress.

1 | Introduction

The m^{6}A modification plays a crucial role in regulating mRNA metabolism and various biological processes by influencing mRNA stability (Visvanathan and Somasundaram 2018), translation efficiency (Wang et al. 2015), alternative splicing (Zhao et al. 2014), and nucleocytoplasmic transport (Roundtree et al. 2017). m^{6}A modification is mainly controlled by m^{6}A methyltransferases (writers), demethylases (erasers) and m^{6}A reading proteins (readers), which add, remove, and recognise m^{6}A modifications, respectively. In Arabidopsis, two types of m^{6}A-writers have been identified, one is a multi-component complex, including MTA (METTL3 homology), MTB (METTL14 homology), FIP37 (WTAP homology), VIR (VIRMA homology), HAKAI (Shen et al. 2016; Vespa et al. 2004; Zhong et al. 2008). The other is FIONA1, a homologue of mammalian methyltransferase METTL16 (Wang et al. 2022).

MTA is one of the earliest methyltransferases discovered in *Arabidopsis thaliana* and is mainly distributed in vigorously

Huihui Wang, Huiyuan Wang, and Yue Jia contributed equally to this study.

Summary statement

- This study reveals that m^{6}A RNA methyltransferases, PheMTA1 and PheMTA2, from moso bamboo play a critical role in regulating root development and enhancing salt tolerance in rice by the identification of target RNAs associated with resistance-related genes.
- The findings provide novel insights into m^{6}A-mediated regulation of stress responses and developmental processes, addressing a gap in understanding the functional roles of m^{6}A modification in plants.

dividing tissues such as reproductive organs, apical meristems, and nascent roots. In Arabidopsis, loss of MTA function disrupts embryonic development at the globular stage, leading to embryonic lethality (Zhong et al. 2008). FIP37, which interacts with MTA, plays a role in maintaining stem meristem proliferation by negatively regulating the mRNA stability of key genes in Arabidopsis. (Shen et al. 2016). Knockout of FIP37 results in delayed endosperm and embryo development, ultimately causing embryonic death (Vespa et al. 2004; Zhong et al. 2008). In addition, mutations of *VIR* and *HIZ2* lead to impaired root growth in plants (Růžička et al. 2017). In rice, OsFIP, a homologue of mammalian WTAP, has been identified as one of the components of the rice m^{6}A methyltransferase complex. OsFIP mediates m^{6}A deposition on transcripts encoding NTPase and threonine proteases, accelerating the degradation of these sporogenesis-related transcripts to regulate microsporogenesis (Zhang et al. 2019). The interaction between OsMTA2 and OseIF3h suggests that OsMTA2 may be involved in OseIF3h-mediated regulation of seedling growth and pollen development (Huang et al. 2021). In strawberries, *MTA* regulates non-hopping fruit ripening through the abscisic acid (ABA) pathway (Zhou, Tang, et al. 2021). The above evidence suggest that m^{6}A writer complex is involved in the regulation of various growth and development processes of plants, including embryonic development (Zhong et al. 2008), root vascular formation (Růžička et al. 2017), seedling growth (Arribas-Hernández et al. 2018), and apical dominance formation (Bodi et al. 2012).

Stressors such as high salinity and drought inhibit plant growth and reduce yield. To survive, plants regulate the expression of stress-responsive genes through various mechanisms. m^{6}A modification plays a critical role in gene regulation under stress conditions. In Arabidopsis, the growth of *vir-1*, *MTB* RNAi, and *hakai* mutants was significantly impaired under salt stress, and the *mta* mutant complemented by *ABI3:MTA* also exhibited slight growth inhibition (Hu et al. 2021). VIR-mediated m^{6}A methylation positively regulates salt tolerance in Arabidopsis by stabilising the mRNA of key salt stress regulators (Hu et al. 2021). Knockdown of *MTA* and *FIP37*, key components of the m^{6}A methyltransferase complex, severely affects the growth of Arabidopsis under low temperatures, with MTA modulating cold tolerance by altering m^{6}A modification and translation efficiency of the cold-responsive gene *DGAT1* (Wang et al. 2023). *FIONA1* affects Arabidopsis salt stress resistance by regulating m^{6}A modification and transcripts stability of stress response genes (Cai et al. 2024). Similarly, *PagFIP37* overexpression improved poplar salt tolerance by modulating salt-responsive genes, including *PagMYB48*, *PagGT2*, and *PagNAC2* (Zhao et al. 2024). In apple, *MdMTA* RNAi plants displayed developmental defects, including weaker roots and shorter plant height, while overexpression of *MdMTA* resulted in no significant changes in root system and plant height but conferred greater drought tolerance (Hou et al. 2022). MdMTA-mediated m^{6}A modification enhances drought resistance in apple by promoting mRNA stability and translation efficiency of genes involved in oxidative stress (Hou et al. 2022). Overexpression of *PtrMTA* in poplar increased trichome density and enhanced root development, leading to improved drought tolerance (Lu et al. 2020). Although extensive research has explored the role of m^{6}A modification mediated by MTA in model plants, the connection between m^{6}A modification and plant growth in moso bamboo remains unclear.

Recently, HyperTRIBE, which integrates the hyperactive E488Q mutant into ADARcd, has been developed. HyperTRIBE uses hyperactive RNA-editing enzymes fused to RNA-binding proteins (RBPs) to identify target RNAs by converting adenosine (A) to inosine (I) near the binding sites (Xu et al. 2018). The hyperactive ADAR significantly enhances editing efficiency, reduces sequence bias, and increases the sensitivity of the technique without compromising specificity. Although RNase-based labelling strategies, such as CLIP, detect binding motifs, HyperTRIBE offers a simpler and more cost-effective method, which is likely to become a key tool for identifying RBP-target RNAs. Using HyperTRIBE, ECT2 and ECT3-bound RNAs were successfully identified in *Arabidopsis thaliana*, with both proteins sharing most of their targets, indicating functional redundancy in vivo, consistent with their similar expression patterns and gene functions (Arribas-Hernandez et al. 2021). Additionally, HyperTRIBE was successfully applied to identify the target RNAs of the stress granule marker UBP1C in Arabidopsis and rice (Yin et al. 2023). It suggests that this technology is effective in plant systems.

In this study, we identified the m^{6}A methyltransferases PheMTA1 and PheMTA2 in moso bamboo and found that they are involved in root development and enhance salt tolerance in rice. Using the HyperTRIBE method, we identified the potential target RNAs bound by PheMTA1 and PheMTA2 in rice. Moreover, we discovered that PheMTA1 and PheMTA2 influence the expression and alternative splicing (AS) of stress-related genes, such as *OsRS33*, *OsPRR73*, and *OsHAP2E*, which promotes root development and improves salt stress resistance in rice.

2 | Materials and Methods

2.1 | Identification of the Bamboo Methyltransferase Gene Family

To identify the m^{6}A methyltransferase gene family in Moso bamboo, we downloaded the conserved HMM domain (PF05063) of the MT-A70 gene family from the Pfam database (Mistry et al. 2021). We conducted a search in the bamboo protein sequences using hmmsearch (Finn et al. 2011) with

default parameters, retaining genes with an E-value less than 1E−5. To infer the evolutionary relationships, we used the protein sequences of MT-A70 family genes from human, rice, Arabidopsis, and the identified MT-A70 family members of *Phyllostachys edulis* to construct a phylogenetic tree using MegaX (Kumar et al. 2018).

2.2 | Genetic Transformation of *PheMTA1* and *PheMTA2* in Rice and Arabidopsis

All transgenic rice plants were generated in the background of Kitaake. The codon of ADARcd^{E488Q} is optimised for enhanced expression in rice and then fused to the C-terminus of *PheMTA1* and *PheMTA2*, respectively. After ligating the fused fragment to the pCUBI 1390 vector, we obtained *UBI$_{PRO}$: PheMTA1-ADARcd^{E488Q}-FLAG* and *UBI$_{PRO}$: PheMTA1-ADARcd^{E488Q}-FLAG*. The recombinant plasmid was transformed into Kitaake calli by *Agrobacterium*-mediated T-DNA insertion. PCR amplification was conducted on genomic DNA using primers of the hygromycin gene to identify positive transgenic rice. RT-qPCR was performed with gene-specific primers to detect the expression of *PheMTA1* and *PheMTA2*. *OsACTIN1* was used as the reference gene (Supporting Information S9: Table S1). We collected the leaves from T0 transgenic rice with high expression and extracted RNA with a Total RNA Extraction Kit (Tiangen, DP#441). RNA-seq was carried out to identify target RNA by detecting A-G mutation sites.

The transgenic Arabidopsis was generated in the background of *rdr6-11*. The ADARcd sequence here was derived from genomic DNA of *Drosophila* that contained 2 introns. We employed the Gateway cloning system to construct *35S$_{PRO}$:GFP-PheMTA1-ADARcd^{Drosophila}* and *35S$_{PRO}$:GFP-PheMTA2-ADARcd^{Drosophila}*. Briefly, the CDS sequences of *PheMTA1* and *PheMTA2* were cloned and inserted into the pGWB505 plasmid. The recombinant plasmid was transformed into Arabidopsis through *Agrobacterium*-mediated transformation of inflorescence. Then, the harmonious lines of Arabidopsis were screened for subsequent experiments.

2.3 | Subcellular Localisation and RT-qPCR

The CDS of *PheMTA1* and *PheMTA2* were cloned and inserted into pCAMBIA1302 vector to generate *35S$_{PRO}$: PheMTA1-GFP* and *35S$_{PRO}$: PheMTA2-GFP* using specific primers (Supporting Information S9: Table S1). The vectors were transformed into *Agrobacterium tumefaciens* GV3101 and subsequently infected into 2-week-old tobacco leaves. After 2–3 days, GFP was detected using fluorescence microscopy with the wavelength from 490 to 553 nm.

Total RNA was extracted from samples using an FastPure Universal Plant Total RNA Isolation Kit (Vazyme, RC411-01). One microgram of total RNA was used to synthesise cDNA using a HiScript III All-in-one RT SuperMix (Vazyme, R333-01). RT-qPCR was performed using HiScript II Q RT SuperMix for qPCR (Vazyme, R222-01) with specific primers (Supporting Information S9: Table S1). For relative gene expression analysis, *Actin* was applied as reference gene and data were analysed with $2^{-\Delta\Delta C_t}$ method.

2.4 | Detection of Resistance to Salt Stress in Transgenic Rice and Arabidopsis

The seeds of T2 generation of transgenic rice were sown in hydroponic boxes, cultured with nutrient solution for 3 weeks. Then seedlings were placed in the nutrient solution containing 150 mM NaCl for 6 days. The growth of the seedlings was observed, and the survival rate was recorded. After that, the solution with NaCl was replaced with normal nutrient solution, and the seedlings continued to grow for 7 days. The wilting of the seedlings was observed, and the survival rate was recorded.

For Arabidopsis, 1/2 MS medium with or without 150 mM NaCl was prepared. The seeds of WT, *ADAR*, *PheMTA1*, *PheMTA2* were sterilised and sown on both 1/2 MS medium and salt stress medium at 22°C (light: darkness = 16 h:8 h). The germination of WT, *ADAR*, *PheMTA1*, *PheMTA2* was recorded during the first week. After 14 days of treatment, the phenotype was observed and the root length of Arabidopsis was measured by imageJ.

2.5 | m^{6}A Dot Blot

The total RNA of each sample was adjusted to three gradients: 2000, 1000, 500 ng/μL. RNA was incubated at 95°C for 5 min and then spotted onto a nitrocellulose membrane. Following cross-linking under a 302 nm UV lamp for 15 min, the membrane was washed with TBST buffer for 5 min. After blocking with 5% skim milk for 1 h, the membrane was washed with TBST buffer for 5 min and subsequently incubated with m^{6}A antibody for 1 h. The membrane was then washed in TBST buffer for 30 min before incubated with IgG antibody for 1 h, followed by another 30-min TBST wash. After incubation with ECL substrate for 1 min, the membrane was exposed in darkroom. Finally, the membrane was stained in a 0.02% methylene blue solution for 30 min and rinsed with ddH_2O.

2.6 | Identifying Target RNAs Bound by PheMTA1 and PheMTA2

The analysis pipeline for identifying target RNAs of PheMTA1 and PheMTA2 was based on the method previously described (Zhou, Niu, et al. 2021). Briefly, transcriptome from *OE-ADAR*, *OE-PheMTA1*, and *OE-PheMTA2* were aligned to the rice genome OsativaKitaake_499_v3.1 (Jain et al. 2019) using Tophat2 (Trapnell et al. 2009) with the following parameters "--library-type fr-firststrand -m 1 -I 50000". Following SNP detection via GATK4 using GATK HaplotypeCaller, GATK GenotypeGVCFs, and GATK VariantFiltration (-window 35 -cluster 3 --filter-name FilterFS --filter-expression "FS > 30.0" --filter-name FilterQD --filter-expression "QD < 2.0"), only A-to-G mutation sites were marked as candidate editing sites of PheMTA1 and PheMTA2. The final editing sites of PheMTA1 and PheMTA2 were obtained by subtracting *OE-ADAR*.

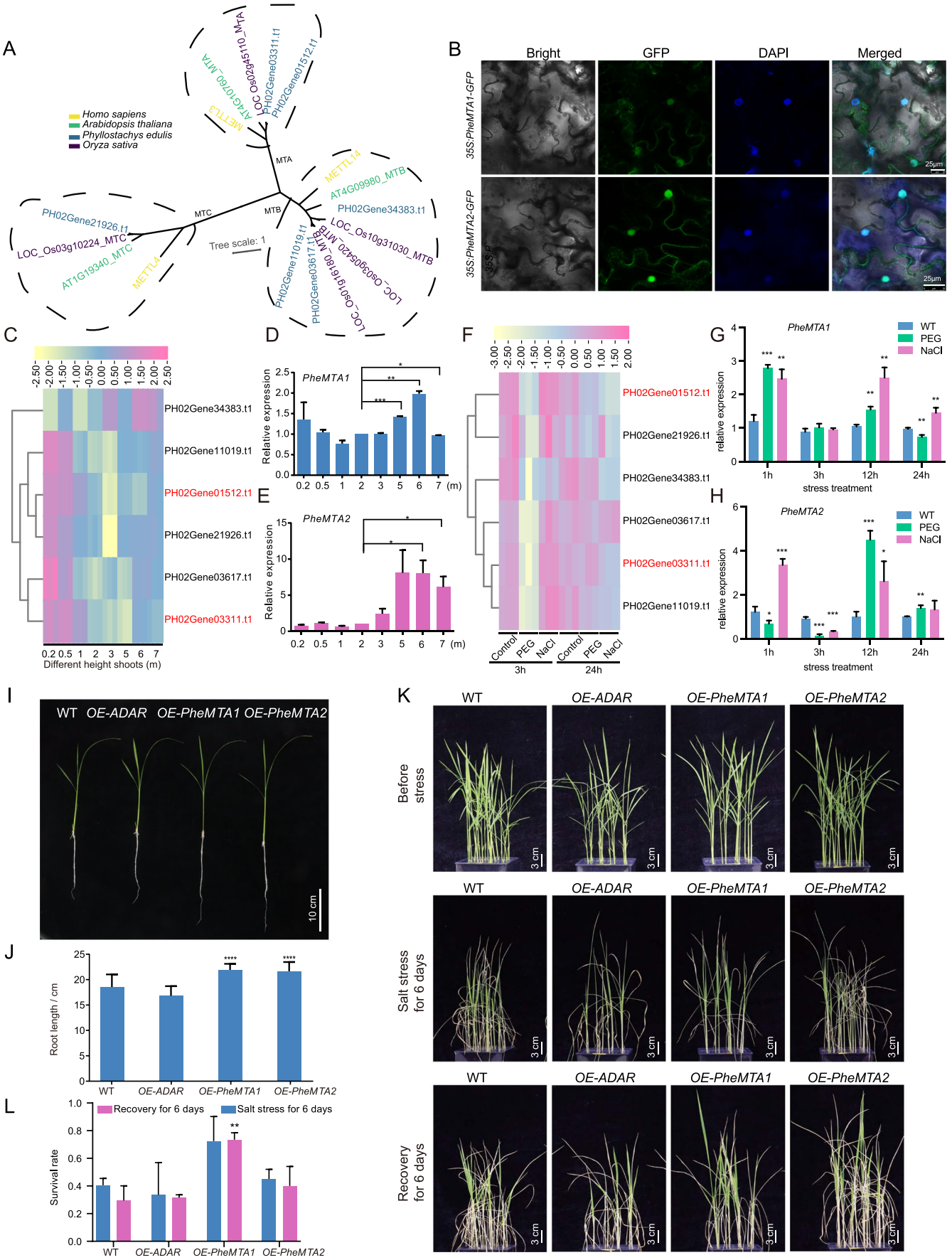

FIGURE 1 | Legend on next page.

2.7 | Differential Gene Expression Analysis and GO Enrichment in Transgenic Rice

We constructed strand-specific RNA-seq libraries using the dUTP method. The raw data were aligned to the reference genome using HISAT2 (Kim et al. 2019) with following parameters "-k 1--rna-strandness RF --dta --n-ceil L,0,0.15". Transcripts per million (TPM) were calculated through StringTie (Pertea et al. 2015) with the following parameters "-e -G $GFF –rf". Differentially expressed genes (DEGs) were identified using DESeq. 2 (Love et al. 2014), applying a *p*-value (*p*-adj) threshold of less than 0.05 and a fold change (FC) greater than 2. GO enrichment analysis was performed using the AgriGO v2.0 database, with significantly enriched terms defined as those having a False Discovery Rate (FDR) less than 0.05. Gene coverage was visualised using IGV (Robinson et al. 2011).

2.8 | Analysis and Validation of Differential Alternative Splicing Events

rMATS (v4.1.2; Shen et al. 2014) was used to detect differential AS events from RNA-Seq with default settings. Four types of AS events were analysed: alternative 5′ splice site (A5SS), alternative 3′ splice site (A3SS), retained intron (RI), and skipped exon (SE). Events with an absolute inclusion level difference (|IncLevelDifference|) greater than 0.05 and an FDR less than 0.05 were considered significant. Visualisation of alternative splicing events was conducted using rmats2sashimiplot (v2.0.2). To validate the differential alternative splicing events via PCR, we designed normal primers that can detect all isoforms of the mRNA of interest (Supporting Information S9: Table S1). The forward primer and reverse primer were located on the upstream and downstream exons of the retained introns, respectively. After that, isoform-specific primers (Supporting Information S9: Table S1) were designed for qPCR to quantify differential AS events. For the intron-retained isoform, forward primer was located on the retained intron. For the intron-spliced isoform, forward primer (20 bp) consists of the last 10 bp of the upstream exon and the first 10 bp of the downstream exon. For relative gene expression analysis, *OsUBQ* was applied as reference gene and data were analysed with $2^{-\Delta\Delta C_t}$ method.

2.9 | RNA Immunoprecipitation Quantitative PCR (RIP-qPCR)

Leaves (3 g) from *OE-ADAR*, *OE-PheMTA1* and *OE-PheMTA2* plants were cut into 2 mm pieces and crosslinking in 1% formaldehyde supplemented with 1 mM PMSF under vacuum at room temperature for 30 min. The crosslinking reaction was stopped by adding glycine solution to a final concentration of 0.1 M for 10 min under vacuum. The fixed leaves were ground into powder and incubated with lysis buffer (150 mM KCl, 50 mM HEPES [pH 7.5], 2 mM EDTA, 1% NP-40, 0.5 mM DTT, 1× cocktail protease inhibitor, and 40 U/mL RNase inhibitor) at 4°C for 30 min. After centrifugation at 13 000 rpm at 4°C for 15 min, the lysates were collected and immunoprecipitated with prewashed Anti-FLAG M2 magnetic beads (Sigma-Aldrich) at 4°C for 4 h. After washing for 4–5 times, the beads were digested by proteinase K at 55°C for 30 min. The RNA was extracted from beads with Trizol and reverse-transcribed into cDNA. The relative enrichment fold was examined via qRT–PCR, with *OsUBQ* used as the internal control.

3 | Results

3.1 | *PheMTA1* and *PheMTA2* Is Involved in Response to Abiotic Stresses in Moso Bamboo

In this study, we investigated the potential function of m^6A methyltransferases in moso bamboo. We classified six MT-A70 family genes in *Phyllostachys edulis* into MTA, MTB, and MTC subfamilies based on phylogenetic analysis (Figure 1A). Previous studies have shown that MTA and MTB in Arabidopsis have the function of methyltransferases, but in rice, only MTA has been confirmed as a methyltransferase (Zhang et al. 2019). In this study, *PheMTA1* (*PH02Gene03311*) and *PheMTA2* (*PH02Gene01512*), which are evolutionarily closest to RNA methyltransferase of human METTL3 and Arabidopsis MTA, were selected for functional analysis. To determine their subcellular localisation, we constructed *35S: PheMTA1-GFP* and *35S: PheMTA2-GFP*, which were transiently expressed in tobacco. Both PheMTA1 and PheMTA2 localised in the nucleus (Figure 1B), consistent with findings in Arabidopsis and rice (Zhang et al. 2019; Zhong et al. 2008).

FIGURE 1 | *PheMTA1* and *PheMTA2* promote root growth and enhance salt tolerance of rice. (A) Phylogenetic tree of the MT-A70 family from human, Arabidopsis, rice, and moso bamboo. (B) Subcellular localisation of PheMTA1 and PheMTA2 in tobacco leaves. Tobacco cells transiently transformed with *PheMTA1* or *PheMTA2* were observed in brightfield and GFP channels, respectively. Nuclei were stained with DAPI. (C) Expression of MT-A70 family genes in bamboo shoots of different heights. Genes marked in red were *PH02Gene03311 (PheMTA1)* and *PH02Gene01512 (PheMTA2)*, while other genes include *PH02Gene21926 (PheMTC)*, *PH02-Gene34383 (PheMTB-1)*, *PH02Gene03617 (PheMTB-2)* and *PH02Gene11019 (PheMTB-3)*. The heatmap colour key ranges from yellow (low expression) to pink (high expression). (D and E) RT-qPCR confirmed the expression of *PheMTA1* (D) and *PheMTA2* (E) in bamboo shoots at different growth stages. Asterisks indicate significant differences (*$p < 0.05$, **$p < 0.01$, *** $p < 0.001$) determined by *t*-test. (F) Expression of MT-A70 family genes in moso bamboo under PEG and salt treatment. (G and H) Expression levels of *PheMTA1* (I) and *PheMTA2* (J) after 1, 3, 12, and 24 h of NaCl treatment and PEG treatment. Data were presented as means ± SD. (*$p < 0.05$, **$p < 0.01$, ***$p < 0.001$, Student's *t*-test, two-tailed). (I) Phenotypes of *OE-PheMTA1* and *OE-PheMTA2* after 3 weeks of cultivation. (J) Root length of *OE-PheMTA1* and *OE-PheMTA2* were measured, and statistical analysis was performed using a *t*-test (**$p < 0.01$). (K) Phenotypes of WT, *OE-ADAR*, *OE-PheMTA1*, *OE-PheMTA2* under salt stress. (L) Survival rate of WT, *OE-ADAR*, *OE-PheMTA1*, *OE-PheMTA2*. The blue bar represents the survival rate after 6 days of salt stress, and the red bar represents survival rate after 6 days of recovery. The experiment was independently repeated three times. Asterisks indicate significant differences (*$p < 0.05$, **$p < 0.01$, ***$p < 0.001$) determined by *t*-test. [Color figure can be viewed at wileyonlinelibrary.com]

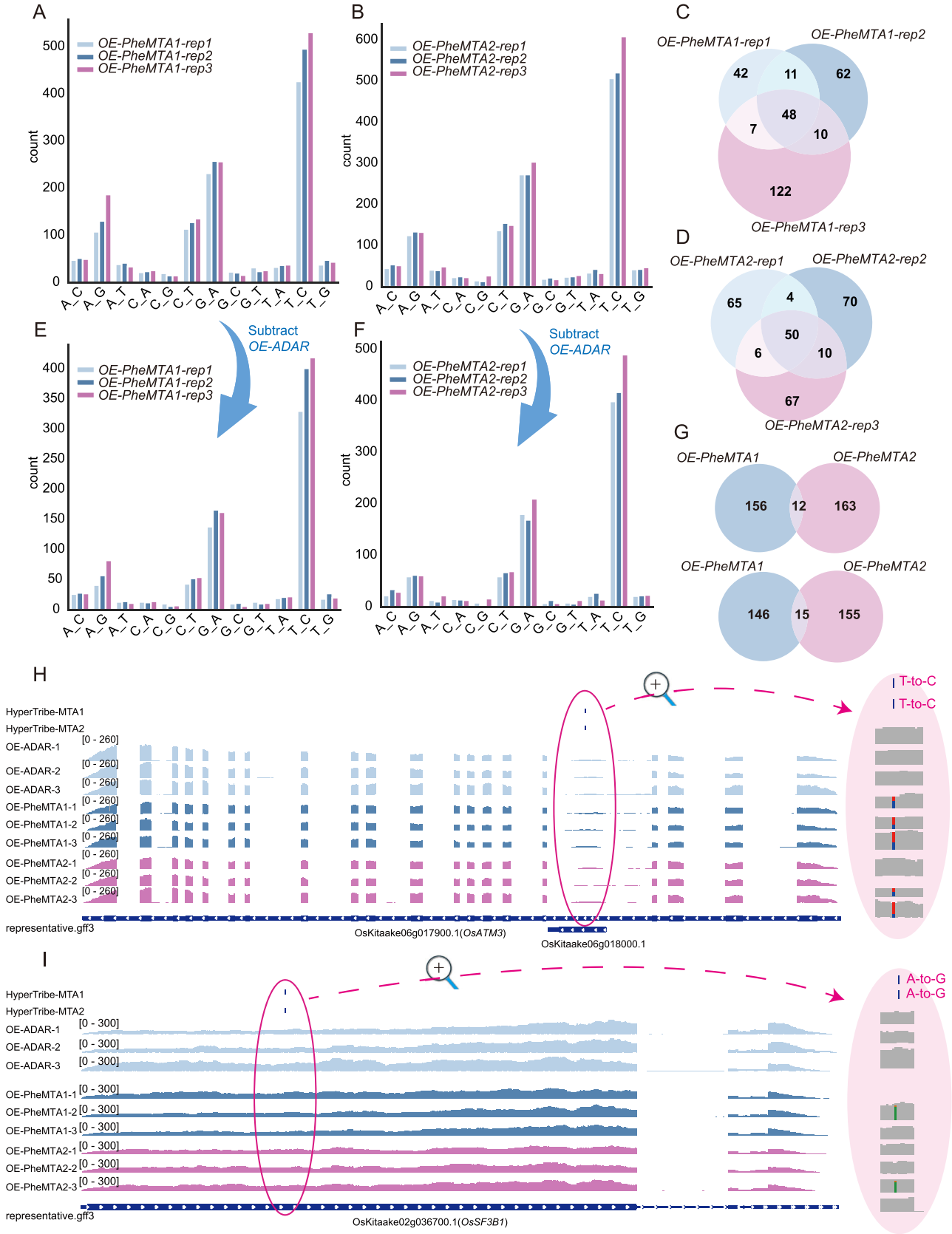

FIGURE 2 | Identification of potential MTA binding sites (A-to-G edit) in *OE-PheMTA1* and *OE-PheMTA2*. (A and B) Distribution of different SNP types in *OE-PheMTA1* (A) and *OE-PheMTA2* (B). (C and D) Overlap of A-to-G editing sites among three independent lines of *OE-PheMTA1* (C) and *OE-PheMTA2* (D). (E and F) The final A-to-G sites in *OE-PheMTA1* (E) and *OE-PheMTA2* (F) after subtracting the editing sites of *OE-ADAR*. (G) The figure shows the overlap of A-to-G sites (12 sites) in *OE-PheMTA1* and *OE-PheMTA2*, and the overlap of target genes (15genes) in *OE-PheMTA1* and *OE-PheMTA2*. (H–I) The wiggle plots show A-to-G sites and gene expression of *OsATM3* (H) and *OsSF3B1* (I). The wiggle plot in the pink circle was enlarged. [Color figure can be viewed at wileyonlinelibrary.com]

Previous studies have revealed the transcriptome profiles of rapid growth (Chen, Sun, et al. 2022) and degradation (Zhang et al. 2024) of bamboo shoots. Using previously published transcriptome data from bamboo (Vasupalli et al. 2021), we examined the expression of MT-A70 family genes during the early growth stages of bamboo shoots. Expression levels were relatively high in bamboo shoots at 0.2 and 0.5 m, gradually decreasing as the shoots grew to 1, 2, and 3 m, before rising again at around 5 m in height (Figure 1C). The expression of *PheMTA1* and *PheMTA2* was further validated by RT-qPCR (Figure 1D,E, Supporting Information S9: Table S1), suggesting that MT-A70 genes, particularly *PheMTA1* and *PheMTA2*, exhibit transcriptional dynamics during bamboo shoot growth and development. Additionally, we found that most MT-A70 genes, including *PheMTA1* and *PheMTA2*, were downregulated after 3 h of PEG treatment or 24 h of salt stress (Figure 1F). *PheMTA1* and *PheMTA2* also responded rapidly to PEG and salt treatment within 1 hour (Figure 1G,H), indicating that MT-A70 genes, especially *PheMTA1* and *PheMTA2*, present transcriptional dynamics during abiotic stress responses in moso bamboo.

3.2 | PheMTA1 and PheMTA2 Promote Root Growth and Improve Salt Tolerance of Rice

To identify the target RNAs bound by PheMTA1 and PheMTA2, we constructed *Ubi:PheMTA1-ADARcd^{E488Q}-FLAG*, *Ubi:PheMTA2-ADARcd^{E488Q}-FLAG*, and *Ubi:ADARcd^{E488Q}-FLAG* vectors (as control) using the HyperTRIBE method. The *ADARcd^{E488Q}* sequence was codon-optimised for rice. These transgenic lines were labelled as *OE-PheMTA1*, *OE-PheMTA2*, and *OE-ADAR*, respectively (Figure S1A). The m^{6}A modification levels in *OE-PheMTA1* transgenic materials were indeed increased, further confirming the methyltransferase activity (Figure S2). Compared to *OE-ADAR*, *OE-PheMTA1* and *OE-PheMTA2* did not show significant differences in leaf length, but their roots were noticeably longer (Figure 1I,J), indicating that *PheMTA1* and *PheMTA2* play a crucial role in rice root development.

Salt stress is a major abiotic factor affecting rice growth and yield. To evaluate the roles of *PheMTA1* and *PheMTA2* under salt stress, 3-week-old hydroponically grown *OE-PheMTA1* and *OE-PheMTA2* were treated with a nutrient solution containing 150 mM NaCl. After 6 days of salt treatment, the vitality of *OE-PheMTA1* and *OE-PheMTA2* was significantly better than that of WT and *OE-ADAR*, and the survival rate of *OE-PheMTA1* and *OE-PheMTA2* was markedly higher than that of WT and *OE-ADAR*. After a 6-day recovery period in nutrient solution, only a few WT and *OE-ADAR* seedlings continued to grow, whereas the majority of *OE-PheMTA1* and *OE-PheMTA2* seedlings recovered and produced new leaves (Figures 1K,L and S3). These results demonstrate that *PheMTA1* and *PheMTA2* promote root growth and positively regulate salt tolerance in rice.

3.3 | Identification of Potential Target RNAs Bound by PheMTA1 and PheMTA2 in Rice

To identify the target mRNAs bound by PheMTA1 and PheMTA2, three lines with high expression levels of *OE-PheMTA1*, *OE-PheMTA2*, and *OE-ADAR* were selected for RNA-seq analysis. Target mRNAs were identified based on A-to-G editing sites. There were 108, 131 and 187 A-to-G editing sites in three lines of *OE-PheMTA1*, respectively (Figure 2A). Similarly, there were 125, 134 and 133 A-to-G editing sites in three lines of *OE-PheMTA2* (Figure 2B). Additionally, the overlap of A-to-G sites among the three lines was 48 for *OE-PheMTA1* and 50 for *OE-PheMTA2*, respectively (Figure 2C,D). After subtracting the editing sites of *OE-ADAR*, we obtained the final A-to-G sites in *OE-PheMTA1* and *OE-PheMTA2* (Figure 2E–G, Supporting Information S9: Tables S2 and S3). Based on the results of HyperTRIBE, we randomly selected one gene targeted by both PheMTA1 and PheMTA2, *OsKitaake05g173400*, and performed RNA Immunoprecipitation quantitative PCR (RIP-qPCR) to validate its binding sites. The result confirmed that *OsKitaake05g173400* was indeed bound by PheMTA1 and PheMTA2, as demonstrated through RIP-qPCR experiments (Figure S4). Among the overlapped 15 genes, *OsATM3* affects apical meristem cell activity. The plant height and lateral root of *osatm3* mutant becomes shorter (Zuo et al. 2017). We found that PheMTA1 and PheMTA2 bind to the site which was located in the overlapping region of *OsATM3* and another gene, *OsKitaake06g018000* (Figure 2H). *OsSF3B1* regulates the splicing of mRNA precursors and the inhibition of splicing increases the susceptibility of seedlings to salt stress in rice (Butt et al. 2021; Butt et al. 2019). We found that PheMTA1 bind to *OsSF3B1* (Figure 2I), which may regulate the splicing of transcripts, resulting in an impact on plant growth and salt resistance.

3.4 | Effects of Overexpressing PheMTA1 and PheMTA2 on Transcription Level of Stress Resistance Genes

To investigate the potential roles of *PheMTA1* and *PheMTA2* in gene regulation, we analysed the gene expression changes in *OE-PheMTA1* and *OE-PheMTA2*. In *OE-PheMTA1*, 428 genes were downregulated, and 2474 genes were upregulated (Figure 3A), while in *OE-PheMTA2*, 1358 genes were downregulated, and 2796 genes were upregulated (Figure 3B, Supporting Information S9: Tables S4 and S5). Further analysis revealed that *PheMTA1* and *PheMTA2* coregulated many genes, with 1387 commonly upregulated genes (Figure 3C) and 156 commonly downregulated genes (Figure 3D). Gene Ontology (GO) enrichment analysis showed that commonly upregulated genes were enriched in oxidation–reduction and response to oxidative stress (Figure 3E). Meanwhile, we found that genes associated with stress response were upregulated in *OE-PheMTA1* and *OE-PheMTA2*. For example, *OsF3'H* inhibits blast infection in rice (Chen, Sun, et al. 2022), and *PIBP1* accumulates in the nucleus to regulate downstream resistance genes *OsWAK14* and *OsPAL1*, enhancing blast resistance in rice (Zhai et al. 2019). *Osrboh7* promotes reactive oxygen species (ROS) production, modulating the immune response (Fan et al. 2018), while *OsGL1-2* strengthens the leaf cuticle, reducing water loss and protecting against drought stress (Islam et al. 2009). As an alkane hydroxylase, *WSL5* catalysers the formation of primary alcohols, participating in epidermal wax biosynthesis, which influences rice drought tolerance (D. Zhang et al. 2020). Additionally, *OsNIA1*, *OsNIA2*, and *OsAPX2* are

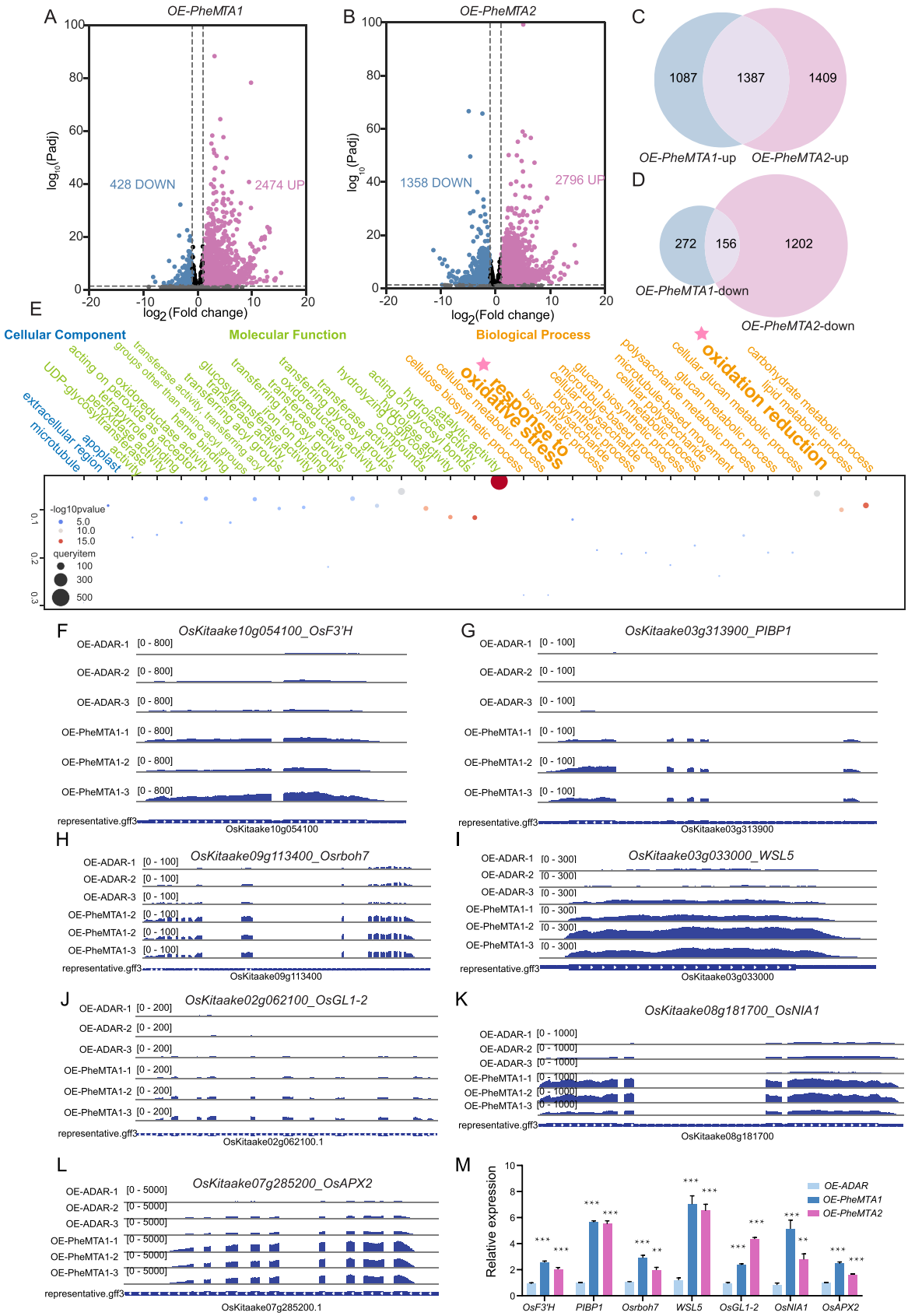

FIGURE 3 | Differentially expressed genes in *OE-PheMTA1* and *OE-PheMTA2*. (A and B) Differentially expressed genes in *OE-PheMTA1* (A) and *OE-PheMTA2* (B). (C and D) Overlap of upregulated genes (C) and downregulated genes (D) induced by *PheMTA1* and *PheMTA2*. (E) GO analysis of common upregulated genes induced by *PheMTA1* and *PheMTA2*. (F–L) The wiggle plots show the expression of *OsF3'H*, *PIBP1*, *Osrboh7*, *WSL5*, *OsGL1-2*, *OsNIA1* and *OsAPX2* in *OE-ADAR*, *OE-PheMTA1* and *OE-PheMTA2*, respectively. (M) RT-qPCR validation of the expression of these genes. Asterisks indicate significant differences (**$p < 0.01$, ***$p < 0.001$) determined by *t*-test. [Color figure can be viewed at wileyonlinelibrary.com]

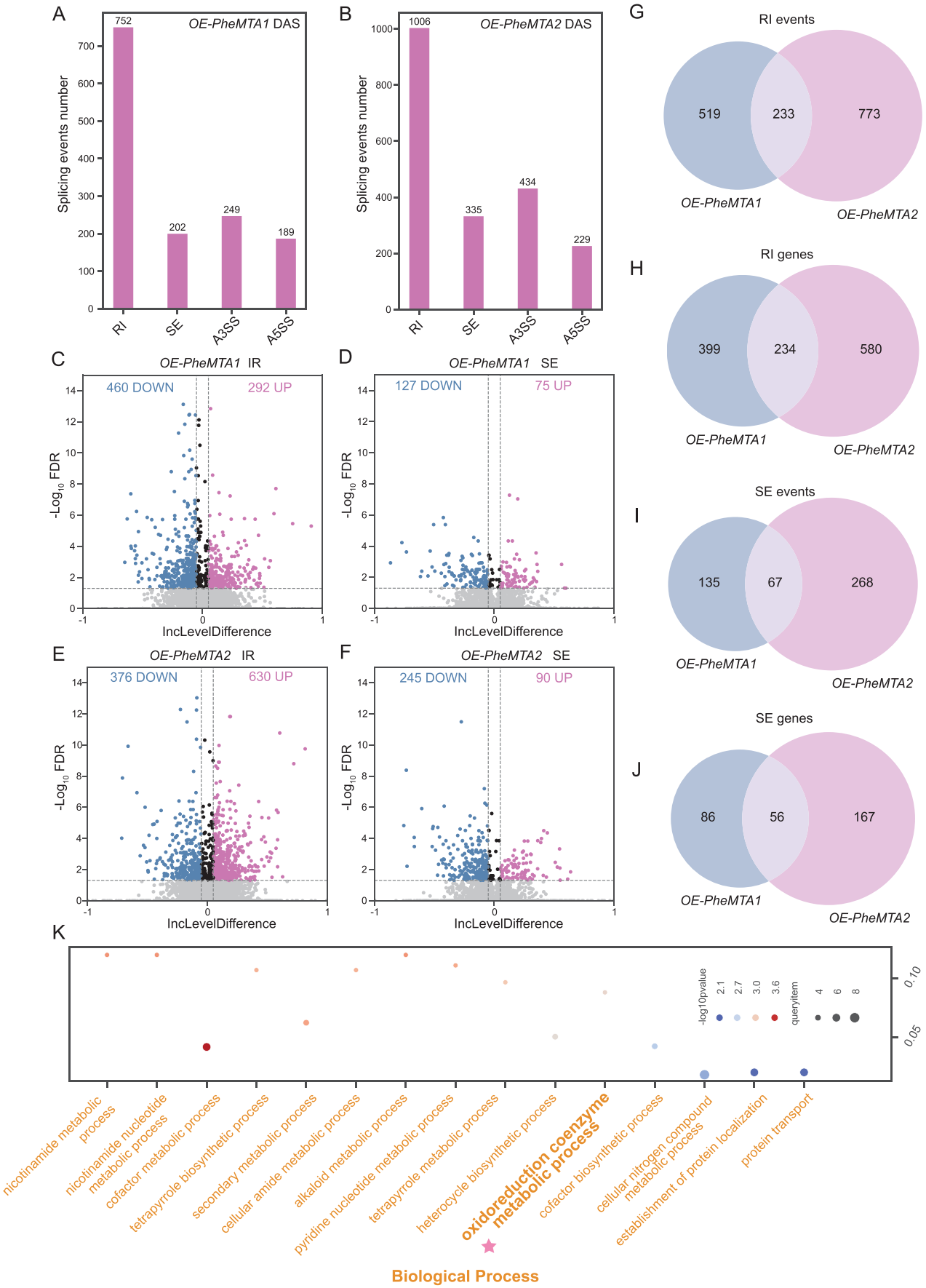

FIGURE 4 | Legend on next page.

associated with salt tolerance in rice (Yi et al. 2022; Zhang et al. 2013). RNA-seq results showed that these stress-related genes were upregulated in *OE-PheMTA1* and *OE-PheMTA2* (Figure 3F–L), which was confirmed by RT-qPCR (Figure 3M, Supporting Information S9: Table S1). These results suggest that *PheMTA1* and *PheMTA2* may enhance salt tolerance by regulating the expression of above stress resistance genes.

3.5 | PheMTA1 and PheMTA2 Effects on the Alternative Splicing of Stress-Related Genes

m^6A methylation influences AS by modulating key spliceosome components or the binding of splicing factors to pre-mRNAs. WTAP and METTL3 are known to regulate gene expression and AS during RNA processing (Ping et al. 2014). To explore the potential roles of *PheMTA1* and *PheMTA2* in RNA processing, we conducted RNA-seq analysis to compare AS events in *OE-PheMTA1* and *OE-PheMTA2*. We identified 1392 and 2004 differential AS events in *OE-PheMTA1* and *OE-PheMTA2*, respectively (Figure 4A,B, Supporting Information S9: Tables S6 and S7), focusing primarily on four AS types: alternative 3′ splice site (A3SS), alternative 5′ splice site (A5SS), retained intron (RI), and skipped exon (SE). There are 123 downregulation and 126 upregulation A3SS events in *OE-PheMTA1* (Figure S5A) and 178 downregulation and 256 upregulation A3SS events in *OE-PheMTA2* (Figure S5A). At the same, we identified 103 downregulation and 86 upregulation A5SS events in *OE-PheMTA1* (Figure S5B) and 127 downregulation and 102 upregulation A5SS events in *OE-PheMTA2* (Figure S5B). Furthermore, several AS events were commonly regulated by both *PheMTA1* and *PheMTA2*, including 81 overlapping A3SS events across 79 genes and 57 overlapping A5SS events across 53 genes (Figure S5C,D). In *OE-PheMTA1*, 460 and 292 introns tended to be spliced and retained, while 127 and 75 exons tended to be skipped and retained, respectively (Figure 4C,D). In *OE-PheMTA2*, 376 and 630 introns tended to be spliced and retained, while 245 and 90 exons tended to be skipped and retained, respectively (Figure 4E,F). Several AS events were regulated by both *PheMTA1* and *PheMTA2*, including 233 RI events in 234 genes and 67 SE events in 56 genes (Figure 4G–J). GO enrichment analysis of genes with differential RI events revealed that they were enriched in oxidoreduction coenzyme metabolic process and other fundamental biological functions (Figure 4K). *OsKitaake12g221800* (*OsMDH12.1*), a gene potentially involved in salt tolerance, showed a preferential exon retention pattern in both *OE-PheMTA1* and *OE-PheMTA2* (Figure S6A). Additionally, *OsKitaake05g280200* (*OsGH3-5*), a gene related to glume and seed development, exhibited a preferential intron spliced pattern in *OE-PheMTA1* and *OE-PheMTA2* (Figure S6B). We confirmed the presence of the predicted isoforms through RT-PCR (Figure S6C,D). It means that *PheMTA1* and *PheMTA2* may play a role in the response to salt stress through AS regulation.

Some genes with differential AS events are associated with stress responses, particularly to high salinity, drought, and disease. The serine/arginine-rich splicing factor OsRS33 plays a role in pre-mRNA splicing and abiotic stress responses in rice. The *rs33* mutant is more sensitive to salt and low-temperature stress (Butt et al. 2022). In *OE-PheMTA1* and *OE-PheMTA2*, the introns of *OsRS33* tended to be retained (Figure 5A). The core transcription factor OsPRR73 is specifically involved in salt stress responses. OsPRR73 binds to the promoter of the sodium-potassium cotransporter *OsHKT2;1* and inhibits its expression by recruiting histone deacetylase HDAC10, preventing excessive sodium ion accumulation and regulating salt tolerance in rice (Wei et al. 2021). In *OE-PheMTA1* and *OE-PheMTA2*, the introns of *OsPRR73* were also retained (Figure 5B). The haem-activating protein OsHAP2E confers salt and drought tolerance as well as resistance to blast fungus in rice. It also enhances photosynthesis and tillering. There were no obvious symptoms of rice overexpressing *OsHAP2E* after inoculation with rice necrosis mosaic virus (RNMV), while the control plants were yellowed and stunted. In *OE-PheMTA1* and *OE-PheMTA2*, the introns of *OsHAP2E* tended to be retained (Figure 5C). The differential AS events of *OsRS33*, *OsPRR73*, and *OsHAP2E* in *OE-PheMTA1* and *OE-PheMTA2* were validated by PCR based on isoform-specific primers (Figure 5D, Supporting Information S9: Table S1), consistent with the RNA-seq results. This suggests that *PheMTA1* and *PheMTA2* may influence salt stress resistance in plants by regulating AS events of stress-related genes.

To investigate whether AS functions as an independent or coordinated layer of gene regulation in *MTA* overexpression lines, we performed an intersection analysis between differential alternative splicing genes (DASG) and differential expressed gene (DEG). In the *OE-PheMTA1* lines, 100 overlapping genes were identified between DASG and DEG, while in the *OE-PheMTA2* lines, 201 overlapping genes were detected (Figure S7). Notably, in *OE-PheMTA1*, both gene expression and AS regulation was observed in salt-regulated genes such as *OsBIPP2C1* and *OsCMO*, as well as in root-regulated genes *OsPTR9* and *Os9BGlu33*. Similarly, in *OE-PheMTA2*, salt-responsive genes (*OsHAP2E*, *OsGF14b*, *OsMADS57*) and root-related genes (*Os9BGlu33*, *OsSPL3*, *OsAGAP*, and *OsAHP1*) were concurrently modulated at the transcriptional and splicing levels. These findings suggest that AS may act either independently or synergistically with gene expression regulation in response to salt stress and root development cues.

In summary, we identified two m^6A methyltransferases in moso bamboo, PheMTA1 and PheMTA2. Overexpression of *PheMTA1* and *PheMTA2* significantly promoted root development and enhanced salt tolerance in rice (Figure 5E). Using the HyperTRIBE method, we fused *PheMTA1* and *PheMTA2* with $ADARcd^{E488Q}$ and introduced them into rice. RNA sequencing (RNA-seq) of

FIGURE 4 | Global identification of differential alternative splicing events in *OE-PheMTA1* and *OE-PheMTA2*. (A and B) The bar chart shows the number of differential AS events in *OE-PheMTA1* (A) and *OE-PheMTA2* (B). (C and D) The volcano plot displays differential intron retention (IR) events in *OE-PheMTA1* (C) and *OE-PheMTA2* (D). IncLevelDifference in *x*-axis presents $IncLevel_{\text{-PheMTA}} - IncLevel_{\text{-ADAR}}$. (E and F) The volcano plot displays differential exon skipping (ES) events in *OE-PheMTA1* (E) and *OE-PheMTA2* (F). (G–J) The Venn diagram shows the intersection of IR event (G) and corresponding gene (H), as well as ES event (I) and corresponding gene (J) between *PheMTA1* and *PheMTA2*. (K) GO enrichment analysis of genes with differential AS events induced by *PheMTA1* and *PheMTA2*. [Color figure can be viewed at wileyonlinelibrary.com]

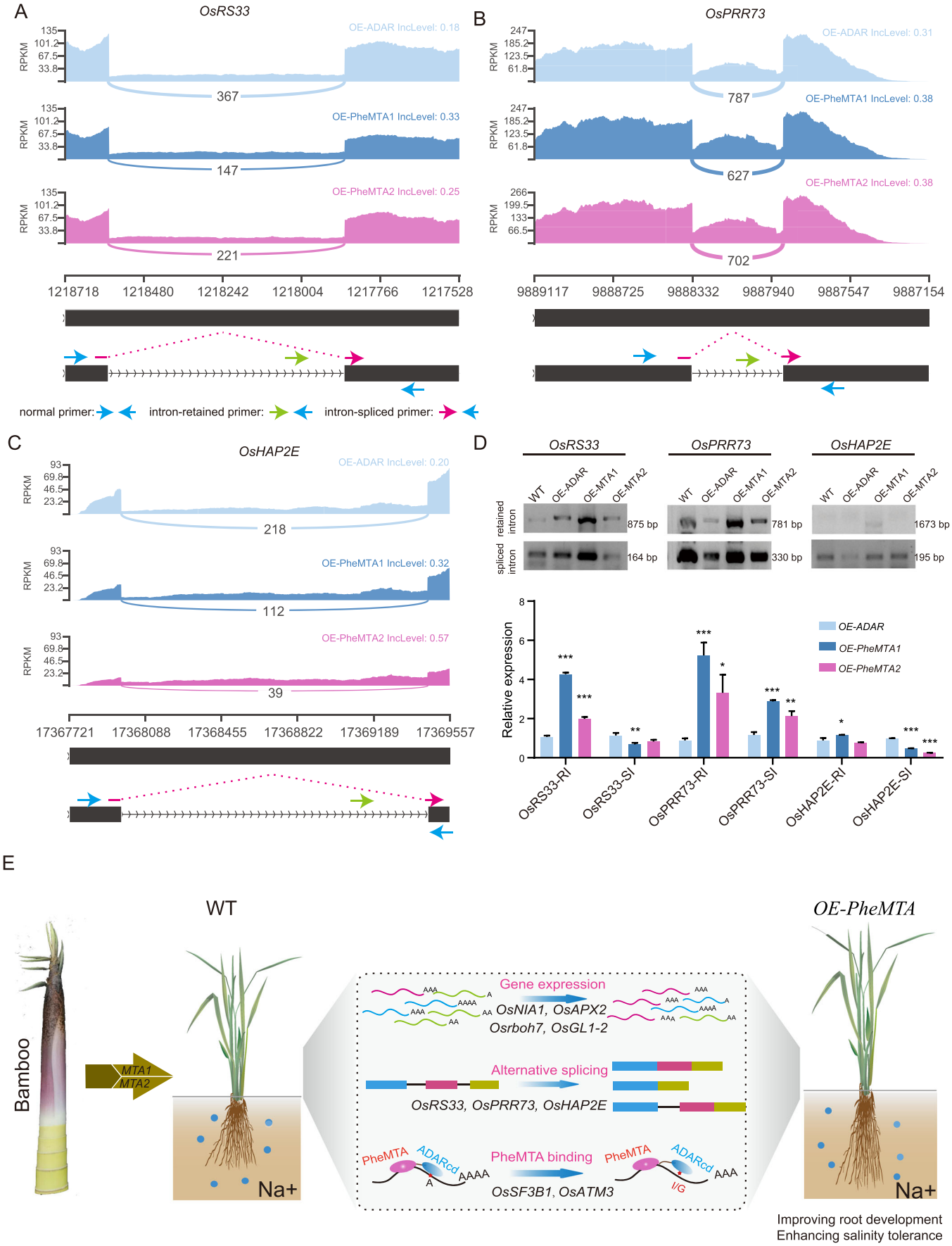

FIGURE 5 | Legend on next page.

the transgenic rice identified the target RNAs bound by PheMTA1 and PheMTA2. PheMTA1 and PheMTA2 bind to *OsATM3* and *OsSF3B1*, which were involved in the development of root and salt resistance. We also revealed the effects of transcription or alternative splicing on resistance-related genes like *OsRS33*, *OsPRR73*, *OsAPX2* and *OsHAP2E*, which are associated with the observed phenotype (Figure 5E).

4 | Discussion

Increasing evidence suggests that m^6A modification is not only related to plant growth and development but also plays a significant role in plant adaptation to various stress environments (Roundtree et al. 2017; Visvanathan and Somasundaram 2018; Wang et al. 2015; Zhao et al. 2014). However, current research primarily focuses on model plants such as *Arabidopsis* and rice, with no relevant reports on the function of m^6A modification in moso bamboo. In this study, we identified two potential methyltransferases, PheMTA1 and PheMTA2, in moso bamboo and transformed them into rice. Our findings revealed that *PheMTA1* and *PheMTA2* promote root elongation and development in rice and enhance salt stress tolerance by influencing the expression and AS events of stress-related genes, such as *OsRS33*, *OsPRR73*, and *OsHAP2E*. To investigate whether this function is conserved across different species, we fused PheMTA1 and PheMTA2 with inactivated ADARcd and transformed them into Arabidopsis. The plants overexpressing *35S:GFP-PheMTA1-ADARcd*^{inactive}, *35S:GFP-PheMTA2-ADARcd*^{inactive}, and *35S:GFP-ADARcd*^{inactive} were labelled as *PheMTA1*, *PheMTA2*, and *ADAR*, respectively (Figure S1B). Next, we observed the phenotypes of *PheMTA1* and *PheMTA2* cultured in 1/2 MS medium for 2 weeks. Compared to *ADAR*, both *PheMTA1* and *PheMTA2* exhibited significantly longer roots, suggesting that *PheMTA1* and *PheMTA2* are key regulators of root development in Arabidopsis (Figure S8A,B). To assess their role in salt stress, *PheMTA1* and *PheMTA2* were sown on 1/2 MS medium containing 150 mM NaCl. We monitored germination over 1–7 days under both normal and salt stress conditions. Under normal conditions, the germination rates of WT, *ADAR*, *PheMTA1*, and *PheMTA2* were similar, reaching nearly 100% at the second day (Figure S8C,D). However, under salt stress, the germination of *PheMTA1* and *PheMTA2* occurred earlier than WT and *ADAR* (Figure S8E). After 2 weeks of salt stress, we found that the survival rate of *PheMTA1* and *PheMTA2* was higher than that of WT and *ADAR*, and their root were significantly longer than WT and *ADAR* (Figure S8F,G). These results indicate that *PheMTA1* and *PheMTA2* promote root growth and positively regulate salt tolerance in Arabidopsis, corroborating their roles in rice as well.

In our attempt to identify the target RNAs bound by PheMTA1 and PheMTA2 in rice with the HyperTRIBE method, no significant enrichment of A-to-G editing events was observed. There was minimal overlap of A-to-G editing sites among the three lines of transgenic rice. We randomly selected *OsKitaake05g173400* targeted by both PheMTA1 and PheMTA2, and validate its binding through RIP-qPCR (Figure S4). In addition, we found that the expression levels of PheMTA1-ADARcd and PheMTA2-ADARcd were low, which may hinder the efficiency of ADAR in RNA editing. Future studies will explore factors influencing ADAR editing efficiency, and efforts will be made to optimise conditions to enhance the performance of the HyperTRIBE method for identification of MTA target sites.

m^6A methyltransferases are involved in plant growth and developmental processes. In Arabidopsis, the knockout of *MTA* causes embryos to arrest at the spherical stage, preventing further development (Zhong et al. 2008). The embryonic lethal phenotype of homozygous *mta* mutants can be rescued by driving *MTA* expression under the embryo-specific ABI3 promoter (Bodi et al. 2012). Additionally, the growth of *vir-1*, *MTB RNAi*, and *hakai* mutants in Arabidopsis is significantly impaired under salt stress, and the *ABI3:MTA* supplemental line also shows slight growth inhibition (Hu et al. 2021). Knockdown of *MTA* and *FIP37*, key components of the m^6A methyltransferase complex, severely affects Arabidopsis growth at low temperatures, with MTA modulating cold tolerance by altering the m^6A modification and translation efficiency of the cold stress-responsive gene *DGAT1* (S. Wang et al. 2023). In rice, *mta2* mutants and *OXMTA2* plants exhibit reduced panicle length, fertility, and effective seed number (Zhang et al. 2019). In strawberries, *MTA* regulates fruit ripening through the abscisic acid (ABA) pathway (Zhou, Tang, et al. 2021). Overexpression of *PtrMTA* in poplar significantly increases trichome density and root development, enhancing drought tolerance (Lu et al. 2020). Similarly, *MdMTA* RNAi plants in apple show developmental defects, including weaker roots and shorter plant height, while *MdMTA*-overexpressing plants show greater drought tolerance despite no significant changes in root system and plant height (Hou et al. 2022). These studies highlight the important role of MTA-mediated m^6A modification in plant development and stress resistance.

In this study, we found that *PheMTA1* and *PheMTA2* significantly promote root growth in Arabidopsis and rice, consistent

FIGURE 5 | Differential alternative splicing events of stress-related genes in *OE-PheMTA1* and *OE-PheMTA2*. (A–C) The wiggle plots show the differential intron retention events of *OsRS33*, *OsPRR73* and *OsHAP2E* in *OE-PheMTA1* and *OE-PheMTA2*. Different tracts represent *OE-ADAR*, *OE-PheMTA1*, and *OE-PheMTA2* from top to bottom. The blue arrows represent common primers that are used to amplify all the isoforms of the interest gene. The green and red arrows represent forward primer of intron-retained isoform and intron-spliced isoform which are used for qPCR, respectively. Isoform-specific reverse primers were the same as normal reverse primers. (D) PCR validation of AS events of *OsRS33*, *OsPRR73* and *OsHAP2E* was performed with common primers respectively. The four lanes in each group represent WT, *OE-ADAR*, *OE-PheMTA1* and *OE-PheMTA2*, respectively. The first row shows intron-retained transcripts, while the second row represents intron-spliced transcripts. The histogram below displays the qPCR validation of the differential RI events using isoform-specific primers. *OsUBQ* was applied as reference gene and data were analysed with $2^{-\Delta\Delta C_t}$ method. Data are given as means ± SD. (*$p < 0.05$, **$p < 0.01$, ***$p < 0.001$, Student's *t*-test, two-tailed). (E) Regulatory model illustrating the role of PheMTA1 and PheMTA2 in rice response to salt stress. *PheMTA1* and *PheMTA2* influence gene expression of *OsNIA1* and *OsAPX2*, and regulate AS events of *OsRS33*, *OsPRR73*, and *OsHAP2E*, thereby affecting plant resistance. [Color figure can be viewed at wileyonlinelibrary.com]

with findings in poplar (Lu et al. 2020). *PheMTA1* and *PheMTA2* enhance salt stress tolerance in rice by upregulating stress-related genes. The m^6A modification levels in *OE-PheMTA1* were indeed increased, confirming the methyltransferase activity of PheMTA1 (Figure S2). However, deep mechanisms of MTA-mediated m^6A modification functioning in root elongation and salt tolerance remains unclear. Further analysis, like revealing differential m^6A modification sites in transgenic plants (*OE-PheMTA1* and *OE-PheMTA2*), will be necessary. In the future, techniques such as Liquid Chromatography-Mass Spectrometry (LC-MS/MS), meRIP-seq, or nanopore direct RNA sequencing could be employed to establish a strong correlation between PheMTA1 and PheMTA2-mediated m^6A modifications and phenotypes.

Acknowledgements

This study was funded by the National Key R&D Program of China (2021YFD2200505), the National Natural Science Foundation of China (32371980), the S&T Innovation (KFB23180) and the Forestry Peak Discipline Construction Project of Fujian Agriculture and Forestry University (72202200205).

Conflicts of Interest

The authors declare no conflicts of interest.

Data Availability Statement

The raw data that supports the findings of this study have been deposited in GSA (https://ngdc.cncb.ac.cn/gsa) under accession CRA019895 (MTA), CRR1084074 (ADAR-mock-29), CRR1084075 (ADAR-mock-33), and CRR1084076 (ADAR-mock-9). The optimised sequences of $ADARcd^{E488Q}$ and $ADARcd^{Drosophila}$ are available in Table S8.

References

Arribas-Hernández, L., S. Bressendorff, M. H. Hansen, C. Poulsen, S. Erdmann, and P. Brodersen. 2018. "An m(6)A-YTH Module Controls Developmental Timing and Morphogenesis in Arabidopsis." *Plant Cell* 30, no. 5: 952–967. https://doi.org/10.1105/tpc.17.00833.

Arribas-Hernandez, L., S. Rennie, M. Schon, et al. 2021. "The YTHDF Proteins ECT2 and ECT3 Bind Largely Overlapping Target Sets and Influence Target mRNA Abundance, Not Alternative Polyadenylation." *eLife* 10: e72377. https://doi.org/10.7554/eLife.72377.

Bodi, Z., S. Zhong, S. Mehra, et al. 2012. "Adenosine Methylation in Arabidopsis mRNA Is Associated With the 3′ End and Reduced Levels Cause Developmental Defects." *Frontiers in Plant Science* 3: 48. https://doi.org/10.3389/fpls.2012.00048.

Butt, H., J. Bazin, S. Alshareef, et al. 2021. "Overlapping Roles of Spliceosomal Components SF3B1 and PHF5A in Rice Splicing Regulation." *Communications Biology* 4, no. 1: 529. https://doi.org/10.1038/s42003-021-02051-y.

Butt, H., J. Bazin, K. V. S. K. Prasad, et al. 2022. "The Rice Serine/Arginine Splicing Factor RS33 Regulates Pre-mRNA Splicing During Abiotic Stress Responses." *Cells* 11, no. 11: 1796. https://doi.org/10.3390/cells11111796.

Butt, H., A. Eid, A. A. Momin, et al. 2019. "CRISPR Directed Evolution of the Spliceosome for Resistance to Splicing Inhibitors." *Genome Biology* 20, no. 1: 73. https://doi.org/10.1186/s13059-019-1680-9.

Cai, J., J. Hu, T. Xu, and H. Kang. 2024. "FIONA1-Mediated mRNA m(6) A Methylation Regulates the Response of Arabidopsis to Salt Stress." *Plant, Cell & Environment* 47, no. 3: 900–912. https://doi.org/10.1111/pce.14807.

Chen, M., L. Guo, M. Ramakrishnan, et al. 2022. "Rapid Growth of Moso Bamboo (*Phyllostachys edulis*): Cellular Roadmaps, Transcriptome Dynamics, and Environmental Factors." *Plant Cell* 34, no. 10: 3577–3610. https://doi.org/10.1093/plcell/koac193.

Chen, S., B. Sun, Z. Shi, X. Miao, and H. Li. 2022. "Identification of the Rice Genes and Metabolites Involved in Dual Resistance Against Brown Planthopper and Rice Blast Fungus." *Plant, Cell & Environment* 45, no. 6: 1914–1929. https://doi.org/10.1111/pce.14321.

Fan, J., P. Bai, Y. Ning, et al. 2018. "The Monocot-Specific Receptor-Like Kinase SDS2 Controls Cell Death and Immunity in Rice." *Cell Host & Microbe* 23, no. 4: 498–510.e5 e495. https://doi.org/10.1016/j.chom.2018.03.003.

Finn, R. D., J. Clements, and S. R. Eddy. 2011. "HMMER Web Server: Interactive Sequence Similarity Searching." *Nucleic Acids Research* 39, no. suppl_2: W29–W37. https://doi.org/10.1093/nar/gkr367.

Hou, N., C. Li, J. He, et al. 2022. "MdMTA-Mediated m(6) A Modification Enhances Drought Tolerance by Promoting mRNA Stability and Translation Efficiency of Genes Involved in Lignin Deposition and Oxidative Stress." *New Phytologist* 234, no. 4: 1294–1314. https://doi.org/10.1111/nph.18069.

Hu, J., J. Cai, S. J. Park, et al. 2021. "N(6)-Methyladenosine mRNA Methylation Is Important for Salt Stress Tolerance in Arabidopsis." *Plant Journal* 106, no. 6: 1759–1775. https://doi.org/10.1111/tpj.15270.

Huang, Y., P. Zheng, X. Liu, H. Chen, and J. Tu. 2021. "OseIF3h Regulates Plant Growth and Pollen Development at Translational Level Presumably Through Interaction With OsMTA2." *Plants (Basel, Switzerland)* 10, no. 6: 1101. https://doi.org/10.3390/plants10061101.

Islam, M. A., H. Du, J. Ning, H. Ye, and L. Xiong. 2009. "Characterization of Glossy1-Homologous Genes in Rice Involved in Leaf Wax Accumulation and Drought Resistance." *Plant Molecular Biology* 70, no. 4: 443–456. https://doi.org/10.1007/s11103-009-9483-0.

Jain, R., J. Jenkins, S. Shu, et al. 2019. "Genome Sequence of the Model Rice Variety Kitaakex." *BMC Genomics* 20, no. 1: 905. https://doi.org/10.1186/s12864-019-6262-4.

Kim, D., J. M. Paggi, C. Park, C. Bennett, and S. L. Salzberg. 2019. "Graph-Based Genome Alignment and Genotyping With HISAT2 and HISAT-Genotype." *Nature Biotechnology* 37, no. 8: 907–915. https://doi.org/10.1038/s41587-019-0201-4.

Kumar, S., G. Stecher, M. Li, C. Knyaz, and K. Tamura. 2018. "MEGA X: Molecular Evolutionary Genetics Analysis Across Computing Platforms." *Molecular Biology and Evolution* 35, no. 6: 1547–1549. https://doi.org/10.1093/molbev/msy096.

Love, M. I., W. Huber, and S. Anders. 2014. "Moderated Estimation of Fold Change and Dispersion for Rna-Seq Data With DESeq.2." *Genome Biology* 15, no. 12: 550. https://doi.org/10.1186/s13059-014-0550-8.

Lu, L., Y. Zhang, Q. He, et al. 2020. "MTA, an RNA m(6)A Methyltransferase, Enhances Drought Tolerance by Regulating the Development of Trichomes and Roots in Poplar." *International Journal of Molecular Sciences* 21, no. 7: 2462. https://doi.org/10.3390/ijms21072462.

Mistry, J., S. Chuguransky, L. Williams, et al. 2021. "Pfam: The Protein Families Database in 2021." *Nucleic Acids Research* 49, no. D1: D412–D419. https://doi.org/10.1093/nar/gkaa913.

Pertea, M., G. M. Pertea, C. M. Antonescu, T. C. Chang, J. T. Mendell, and S. L. Salzberg. 2015. "Stringtie Enables Improved Reconstruction of a Transcriptome From RNA-Seq Reads." *Nature Biotechnology* 33, no. 3: 290–295. https://doi.org/10.1038/nbt.3122.

Ping, X. L., B. F. Sun, L. Wang, et al. 2014. "Mammalian WTAP Is a Regulatory Subunit of the RNA N6-Methyladenosine Methyltransferase." *Cell Research* 24, no. 2: 177–189. https://doi.org/10.1038/cr.2014.3.

Robinson, J. T., H. Thorvaldsdóttir, W. Winckler, et al. 2011. "Integrative Genomics Viewer." *Nature Biotechnology* 29, no. 1: 24–26. https://doi.org/10.1038/nbt.1754.

Roundtree, I. A., G. Z. Luo, Z. Zhang, et al. 2017. "YTHDC1 Mediates Nuclear Export of N(6)-Methyladenosine Methylated mRNAs." *eLife* 6: e31311. https://doi.org/10.7554/eLife.31311.

Růžička, K., M. Zhang, A. Campilho, et al. 2017. "Identification of Factors Required for m(6) A mRNA Methylation in Arabidopsis Reveals a Role for the Conserved E3 Ubiquitin Ligase HAKAI." *New Phytologist* 215, no. 1: 157–172. https://doi.org/10.1111/nph.14586.

Shen, L., Z. Liang, X. Gu, et al. 2016. "N(6)-Methyladenosine RNA Modification Regulates Shoot Stem Cell Fate in Arabidopsis." *Developmental Cell* 38, no. 2: 186–200. https://doi.org/10.1016/j.devcel.2016.06.008.

Shen, S., J. W. Park, Z. Lu, et al. 2014. "rMATS: Robust and Flexible Detection of Differential Alternative Splicing From Replicate RNA-Seq Data." *Proceedings of the National Academy of Sciences* 111, no. 51: E5593–E5601. https://doi.org/10.1073/pnas.1419161111.

Trapnell, C., L. Pachter, and S. L. Salzberg. 2009. "TopHat: Discovering Splice Junctions With RNA-Seq." *Bioinformatics* 25, no. 9: 1105–1111.

Vasupalli, N., D. Hou, R. M. Singh, et al. 2021. "Homo- and Hetero-Dimers of CAD Enzymes Regulate Lignification and Abiotic Stress Response in Moso Bamboo." *International Journal of Molecular Sciences* 22, no. 23: 12917. https://doi.org/10.3390/ijms222312917.

Vespa, L., G. Vachon, F. Berger, D. Perazza, J. D. Faure, and M. Herzog. 2004. "The Immunophilin-Interacting Protein AtFIP37 From Arabidopsis Is Essential for Plant Development and Is Involved in Trichome Endoreduplication." *Plant Physiology* 134, no. 4: 1283–1292. https://doi.org/10.1104/pp.103.028050.

Visvanathan, A., and K. Somasundaram. 2018. "mRNA Traffic Control Reviewed: N6-Methyladenosine (m_6A) Takes the Driver's Seat." *BioEssays* 40, no. 1: 1700093. https://doi.org/10.1002/bies.201700093.

Wang, C., J. Yang, P. Song, et al. 2022. "FIONA1 Is an RNA N(6)-Methyladenosine Methyltransferase Affecting Arabidopsis Photomorphogenesis and Flowering." *Genome Biology* 23, no. 1: 40. https://doi.org/10.1186/s13059-022-02612-2.

Wang, S., H. Wang, Z. Xu, et al. 2023. "m6A mRNA Modification Promotes Chilling Tolerance and Modulates Gene Translation Efficiency in Arabidopsis." *Plant Physiology* 192, no. 2: 1466–1482. https://doi.org/10.1093/plphys/kiad112.

Wang, X., B. S. Zhao, I. A. Roundtree, et al. 2015. "N(6)-methyladenosine Modulates Messenger RNA Translation Efficiency." *Cell* 161, no. 6: 1388–1399. https://doi.org/10.1016/j.cell.2015.05.014.

Wei, H., X. Wang, Y. He, H. Xu, and L. Wang. 2021. "Clock Component OsPRR73 Positively Regulates Rice Salt Tolerance by Modulating OsHKT2;1-Mediated Sodium Homeostasis." *EMBO Journal* 40, no. 3: e105086. https://doi.org/10.15252/embj.2020105086.

Xu, W., R. Rahman, and M. Rosbash. 2018. "Mechanistic Implications of Enhanced Editing by a Hypertribe Rna-Binding Protein." *RNA* 24, no. 2: 173–182. https://doi.org/10.1261/rna.064691.117.

Yi, Y., Y. Peng, T. Song, et al. 2022. "NLP2-NR Module Associated NO Is Involved in Regulating Seed Germination in Rice Under Salt Stress." *Plants (Basel, Switzerland)* 11, no. 6: 795. https://doi.org/10.3390/plants11060795.

Yin, S., Y. Chen, Y. Chen, L. Xiong, and K. Xie. 2023. "Genome-Wide Profiling of Rice Double-Stranded RNA-Binding Protein 1-Associated RNAs by Targeted RNA Editing." *Plant Physiology* 192, no. 2: 805–820. https://doi.org/10.1093/plphys/kiad158.

Zhai, K., Y. Deng, D. Liang, et al. 2019. "RRM Transcription Factors Interact With NLRs and Regulate Broad-Spectrum Blast Resistance in Rice." *Molecular Cell* 74, no. 5: 996–1009.e7. https://doi.org/10.1016/j.molcel.2019.03.013.

Zhang, D., H. Yang, X. Wang, et al. 2020. "Cytochrome P450 Family Member CYP96B5 Hydroxylates Alkanes to Primary Alcohols and Is Involved in Rice Leaf Cuticular Wax Synthesis." *New Phytologist* 225, no. 5: 2094–2107. https://doi.org/10.1111/nph.16267.

Zhang, F., Y. C. Zhang, J. Y. Liao, et al. 2019. "The Subunit of RNA N6-Methyladenosine Methyltransferase OsFIP Regulates Early Degeneration of Microspores in Rice." *PLoS Genetics* 15, no. 5: e1008120. https://doi.org/10.1371/journal.pgen.1008120.

Zhang, W., M. Shi, K. Yang, et al. 2024. "Regulatory Networks of Senescence-Associated Gene-Transcription Factors Promote Degradation in Moso Bamboo Shoots." *Plant, Cell & Environment* 47, no. 9: 3654–3667. https://doi.org/10.1111/pce.14950.

Zhang, Z., Q. Zhang, J. Wu, et al. 2013. "Gene Knockout Study Reveals That Cytosolic Ascorbate Peroxidase 2(OsAPX2) Plays a Critical Role in Growth and Reproduction in Rice Under Drought, Salt and Cold Stresses." *PLoS One* 8, no. 2: e57472. https://doi.org/10.1371/journal.pone.0057472.

Zhao, X., Y. Yang, B. F. Sun, et al. 2014. "FTO-Dependent Demethylation of N6-Methyladenosine Regulates mRNA Splicing and Is Required for Adipogenesis." *Cell Research* 24, no. 12: 1403–1419. https://doi.org/10.1038/cr.2014.151.

Zhao, Y., K. J. Han, Y. T. Tian, et al. 2024. "N(6)-Methyladenosine mRNA Methylation Positively Regulated the Response of Poplar to Salt Stress." *Plant, Cell & Environment* 47, no. 5: 1797–1812. https://doi.org/10.1111/pce.14844.

Zhong, S., H. Li, Z. Bodi, et al. 2008. "MTA Is an Arabidopsis Messenger RNA Adenosine Methylase and Interacts With a Homolog of a Sex-Specific Splicing Factor." *Plant Cell* 20, no. 5: 1278–1288. https://doi.org/10.1105/tpc.108.058883.

Zhou, G., R. Niu, Y. Zhou, et al. 2021. "Proximity Editing to Identify RNAs in Phase-Separated RNA Binding Protein Condensates." *Cell Discovery* 7, no. 1: 72. https://doi.org/10.1038/s41421-021-00288-9.

Zhou, L., R. Tang, X. Li, S. Tian, B. Li, and G. Qin. 2021. "N(6)-Methyladenosine RNA Modification Regulates Strawberry Fruit Ripening in an ABA-Dependent Manner." *Genome Biology* 22, no. 1: 168. https://doi.org/10.1186/s13059-021-02385-0.

Zuo, J., Z. Wu, Y. Li, et al. 2017. "Mitochondrial ABC Transporter ATM3 Is Essential for Cytosolic Iron-Sulfur Cluster Assembly." *Plant Physiology* 173, no. 4: 2096–2109. https://doi.org/10.1104/pp.16.01760.

Supporting Information

Additional supporting information can be found online in the Supporting Information section.